The magnetic properties of disordered Fe–Al alloy system

A. Oubelkacem [a], I. Essaoudi [a], A. Ainane [a,b,*], F. Dujardin [c], J. Ricardo de Sousa [d], M. Saber [a,b]

[a] *Laboratoire de Physique des Matériaux et Modélisation des Systèmes, Unité Associée au CNRST, University of Moulay Ismail, Faculty of Sciences, Physics Department, B.P. 11201, Meknes, Morocco*

[b] *Max-Planck-Institut für Physik Complexer Systeme, Nöthnitzer Str. 38, D-01187 Dresden, Germany*

[c] *Laboratoire de Physique des Milieux Denses (LPMD) Institut de Chimie, Physique et Matériaux (ICPM), 1 Bd. Arago, 57070, Metz, France*

[d] *Departamento de Fisica, Universidade Federal de Amazonas, 69077-000, Manaus-AM, Brazil*

A R T I C L E   I N F O

A B S T R A C T

Using the effective field theory with a probability distribution technique that accounts for the self-spin correlation functions, the magnetic properties of disordered Fe–Al alloys on the basis of a site-diluted quantum Heisenberg spin model are examined. We calculated the critical temperature and the hysteresis loops for this system. We find a number of characteristic phenomena. In particular, the effect of concentration c of magnetic atoms and the reduced exchange anisotropic parameter η on both the critical temperature and magnetization profiles are clarified.

1. Introduction

Magnetic systems have always been of great practical interest, mainly due to their possible usage in information technology, as well as novel materials for a variety of applications. In the former case, the giant magnetoresistance is a special example for technological information storage [1,2]. These materials have also been the subject of intense theoretical investigation in both, pure and disordered versions [3]. Among the family of magnetic alloys, the Fe–Al system has been one of the most interesting because of the several magnetic phases that can be present in this system, such as ferromagnetism, paramagnetism, and even the spin-glass phase [4,5]. The region of the magnetic phase diagram in which these phases exist are strongly dependent upon how the constituent atoms are distributed in the crystalline lattice. The $Fe_{1-q}Al_q$ system in the bcc structure shows an interesting magnetic behavior since its critical temperature decreases with $q = 1 - c$ but shows a kind of plateau for low Al concentrations. Theoretical studies [5,6], using mean field renormalization group [7] and Bogoliubov inequality [8] approaches have been used to explain this behavior by taking a simple Ising Hamiltonian. Sato and Arrot [9] obtained the magnetization by assuming a ferromagnetic exchange between nearest-neighbor Fe atoms and an antiferromagnetic superexchange between two Fe atoms separated by an Al atom. This model, however, predicts an antiferromagnetic phase at low temperatures which was not revealed by neutron scattering experiments [10]. Shukla and Wortis [11] and Grest [12] did their estimates assuming a spin-glass state near the critical Al concentration. In this case, a rather good agreement with experimental data has been achieved. More recently, an experimental study of Fe–Al alloys in the disordered phase has been reported for Al concentrations $q = 1 - c$ with c is the concentration of Fe atoms, in the range $0 \leq q \leq 0.5$ [13]. It has been shown that this system, at room temperature, undergoes a ferro-to paramagnetic phase transition at a critical Al concentration $q_c = 0.475$ [13]. It has also been noted that the critical temperature of the ferro- to paramagnetic transition decreases as the Al concentration increases. Moreover, these alloys

* Corresponding author at: Laboratoire de Physique des Matériaux et Modélisation des Systèmes, Unité Associée au CNRST, University of Moulay Ismail, Faculty of Sciences, Physics Department, B.P. 11201, Meknes, Morocco. Tel.: +212 5 35439482; fax: +212 5 35536808.
  E-mail address: ainane@pks.mpg.de (A. Ainane).

are all ferromagnetic and do not show the anomalous behavior of the ordered ones. Moreno and Montenegro [14] reported an investigation of the ferromagnetic disordered $Fe_{1-q}Al_q$ alloys by magnetization measurements. For a special value of concentration q, they obtained the critical temperature and critical exponents for different alloys. Our aim in this paper is to extend the results reported in Ref. [15] for studying the phase transition and the site-diluted quantum Heisenberg spin model applied to the magnetic properties of Fe–Al disordered alloys, in the framework of the effective field theory with a probability distribution technique [16]. The model studied is the same as that analyzed in Ref. [15]. In particular, an anisotropic Heisenberg model with site dilution is investigated in mean-field approximation. To simplify the consideration further a two-site cluster approximation is already used which is based on a two-site cluster theory introduced by Bobak and Jascur [17] in which attention is focused on a cluster comprising just two selected Heisenberg spins. The magnetic properties such as the hysteresis loops and coercive field as functions of the temperature and concentration respectively are discussed. We discuss on simple cubic symmetric with nearest-neighbor exchange interactions in which the strength is assumed to be different from the bulk value in the surface. In Section 2, we outline the formalism and derive the equations that determine the phase diagrams, the hysteresis loops and critical temperature. The phase diagram of the system as functions of the parameters R, η and c are discussed in Section 3. The conclusion is given in Section 4.

2. Formalism

In order to obtain the critical properties of the Fe–Al disordered alloys we assume a quenched site-diluted quantum Heisenberg model with only the nearest-neighbor interactions. The model is defined on a simple cubic lattice and the Hamiltonian of the system is given by

$$H = -\sum_{\langle ij \rangle} J_{ij} c_i c_j (\xi S_{i,x} S_{j,x} + \eta S_{i,y} S_{j,y} + \zeta S_{i,z} S_{j,z}) \tag{1}$$

where c_i is a random variable which takes the value 1 or 0 according to whether the site i is occupied by a spin S_i, or not. J_{ij} is the exchange parameter between spins. The parameters ξ, η and ζ control the anisotropy of the exchange interaction J_{ij}. For some special values of ξ, η and ζ one recovers the well-known models, namely, the Ising model [I] ($\xi = \eta = 0$), the isotropic Heisenberg model [H] ($\xi = \eta = \zeta$) and the X–Y model [XY] ($\xi = \eta$, $\zeta = 0$).

In this paper we report results for the two-site cluster approximation. The following notation will be adopted throughout. The two nearest-neighboring sites forming the pair cluster are denoted by 1 and 2. λ_i ($i = 1$ to N_1) denote the nearest-neighboring sites of 1 (excluding 2), while α_i ($i = 1$ to N_2) those of 2 (excluding 1). Some lattices have sites common to both the sets $\{\lambda_i\}$ and $\{\alpha_i\}$. These are denoted by $\varphi_i (i = 1$ to $N)$. $\{\lambda_i'\}$ and $\{\alpha_i'\}$ denote the sets $\{\lambda_i\}$ and $\{\alpha_i\}$ when the sets $\{\varphi_i\}$ have been removed. $S_{i,z}$, $S_{i,x}$ and $S_{i,y}$ denote the Pauli matrices which are the components of the quantum spin $\overrightarrow{S_i}$ of magnitude $S = 1/2$ at site i, and the summation runs over all pairs of nearest neighbors.

The starting point for the two-site cluster approximation is to split the Hamiltonian into the following terms

$$H = H_{12} + H_1 + H_2 + H' = H_0 + H' \tag{2}$$

with

$$H_{12} = -c_1 c_2 J \left(\xi S_{1,x} S_{2,x} + \eta S_{1,y} S_{2,y} + \zeta S_{1,z} S_{2,z} \right) \tag{3}$$

and $H_1(H_2)$ is the Hamiltonian type, namely

$$H_1 = -Jc_1 \left(\xi S_{1,x} \sum_{i=1}^{N_1} c_{\lambda_i} S_{\lambda_i,x} + \eta S_{1,y} \sum_{i=1}^{N_1} c_{\lambda_i} S_{\lambda_i,y} + \zeta S_{1,z} \sum_{i=1}^{N_1} c_{\lambda_i} S_{\lambda_i,z} \right) \tag{4}$$

$$H_2 = -Jc_2 \left(\xi S_{2,x} \sum_{i=1}^{N_2} c_{\alpha_i} S_{\alpha_i,x} + \eta S_{2,y} \sum_{i=1}^{N_2} c_{\alpha_i} S_{\alpha_i,y} + \zeta S_{2,z} \sum_{i=1}^{N_2} c_{\alpha_i} S_{\alpha_i,z} \right). \tag{5}$$

Allowing for the fact that H_0 and H' do not commute, the thermal average of $S_{1,z}$, for example, can be written as
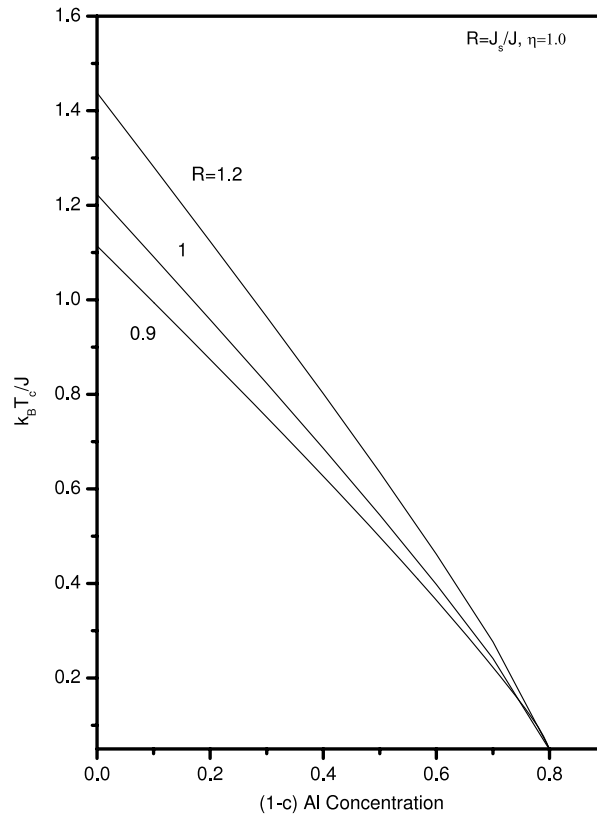
$$\langle S_z \rangle = \left\langle \frac{B}{A} \right\rangle - \left\langle \left(\frac{B}{A} - S_{1,z} \right) \Delta \right\rangle, \tag{6}$$

where

$$A = Tr^0 \exp(-\beta H_0), \qquad B = Tr^0 [S_{1,z} \exp(-\beta H_0)], \tag{7}$$

$$\Delta = 1 - \exp(-\beta H_0) \exp(-\beta H') \exp(\beta H_0). \tag{8}$$

In the above, Tr^0 means the partial trace with respect to the states of the cluster spins S_1 and S_2. Eq. (6) is an exact relation, but is difficult to the presence of the second thermal on the right-hand side. Following Ref. [18], we avoid this difficulty by

Fig. 1. Dependence of the Curie temperature on the $(1 - c)$ Al concentration for different values of the parameter $R = J_s/J$ and for the Heisenberg model $\eta = 1.0$.

replacing the quantum spins surrounding the two-site cluster by Ising spins. With this replacement, H_0 and H' commute and $\Delta \to 0$, so we are left with the simple relation

$$\langle S_z \rangle = \frac{1}{2} \left\langle \frac{Tr^0\{(S_{1,z} + S_{2,z}) \exp[-\beta(H_{12,z} + H_{1,z} + H_{2,z})]\}}{Tr^0 \exp[-\beta(H_{12,z} + H_{1,z} + H_{2,z})]} \right\rangle \tag{9}$$

where

$$H_{1,z} = -x_1 J c_1 S_{1,z} \quad \left(x_1 \equiv \zeta \sum_{i=1}^{N_1} c_{\lambda_i} S_{\lambda_i,z} \right) \tag{10}$$

$$H_{2,z} = -x_2 J c_2 S_{2,z} \quad \left(x_2 \equiv \zeta \sum_{i=1}^{N_2} c_{\alpha_i} S_{\alpha_i,z} \right). \tag{11}$$

Remembering that $c_1^2 = c_1$, etc., on effecting the partial traces in Eq. (9), one has the following result

$$\langle S_z \rangle = c_1 c_2 \left[\langle f_3(x_1, x_2) \rangle + \langle f_2(x_1, x_2) \rangle \right] + 2c_1(1 - c_2) \langle f_1(x_1) \rangle, \tag{12}$$

where

$$f_1(x_1) = \frac{1}{4} \tanh\left(\frac{1}{2} \beta J x_1 \right), \tag{13}$$

$$f_2(x_1, x_2) = \frac{x_1 + x_2}{X} \frac{\sinh\left(\frac{1}{4} \beta J X \right)}{\cosh\left(\frac{1}{4} \beta J X \right) + \exp\left(\frac{1}{2} \beta J \zeta \right) \cosh\left(\frac{1}{4} \beta J Y \right)}, \tag{14}$$

$$f_3(x_1, x_2) = \frac{x_1 - x_2}{Y} \frac{\exp\left(\frac{1}{2} \beta J \zeta \right) \sinh\left(\frac{1}{4} \beta J Y \right)}{\cosh\left(\frac{1}{4} \beta J X \right) + \exp\left(\frac{1}{2} \beta J \zeta \right) \cosh\left(\frac{1}{4} \beta J Y \right)} \tag{15}$$
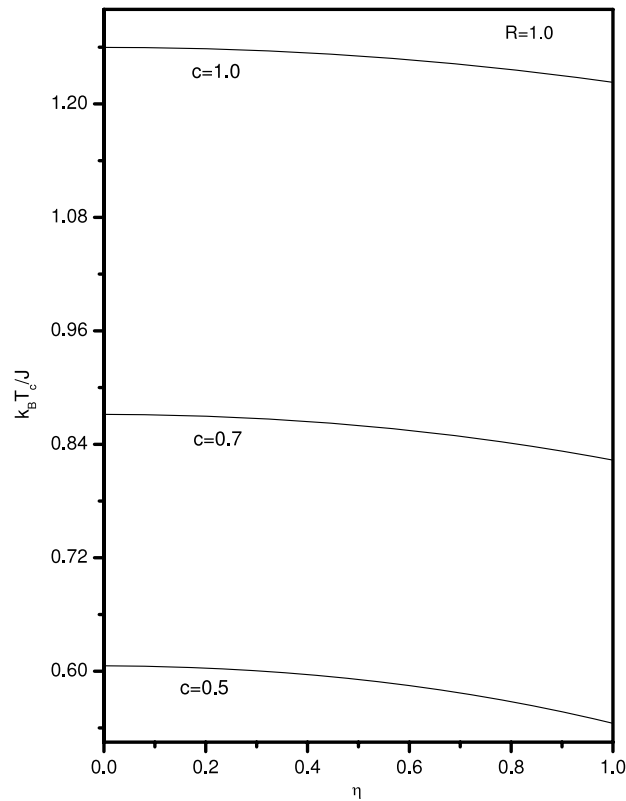
Fig. 2. Dependence of the Curie temperature on the reduced exchange anisotropic parameter η for different values of concentration c.

with

$$X = \sqrt{4(x_1 + x_2)^2 + (\xi - \eta)^2}, \qquad Y = \sqrt{4(x_1 - x_2)^2 + (\xi + \eta)^2}. \tag{16}$$

For the system under consideration, in the case when the exchange interactions are between nearest-neighbor sites only, one finds (for fixed spatial configuration of the spins) and for simplicity the expression of the $\langle S_z \rangle$ as follows

$$\langle S_z \rangle = c \left\langle f_2 \left(\sum_{i_1 \neq 1} J_{i_1 j} c_{i_1} S_{i_1,z}, \sum_{i_2 \neq 1} J_{i_2 j} c_{i_2} S_{i_2,z} \right) \right\rangle \tag{17}$$

where in particular

$$f_2(x_1, x_2) = f_z(x_1, x_2) = \frac{1}{2} \frac{\sinh\left(\frac{1}{2}\beta J(x_1 + x_2)\right)}{\cosh\left(\frac{1}{2}\beta J(x_1 + x_2)\right) + \exp\left(\frac{1}{2}\beta J\right) \cosh\left[\frac{1}{2}\beta J \sqrt{(x_1 - x_2)^2 + \eta^2}\right]}. \tag{18}$$

The sums in Eq. (17) are over the $N - 1$ nearest neighbors of the sites $\overrightarrow{S_1}$ and $\overrightarrow{(S_2)}$, N being the nearest-neighbor coordination number of the lattice.

The method we use is the effective-field theory, fully described in Ref. [16], that employed the probability distribution technique to account for the single-site spin correlations. Following that procedure, we find in the current situation for a fixed configuration of neighboring spins that the layer magnetization is given by

$$m_{nz} = \langle S_{nz} \rangle = \left\langle f_z \left(\sum_{i1 \neq 1} J_{ij} c_{i1} S_{i1,z}, \sum_{i1 \neq 1} J_{ij} c_{i2} S_{i2,z} \right) \right\rangle \tag{19}$$

with $\beta = \frac{1}{k_B T}$ and T is the temperature. In Eq. (19), $\langle \cdots \rangle$ indicates the usual canonical ensemble thermal average for a given configuration and the sum runs over all nearest neighbors of the spin $\overrightarrow{S}_i$.

To perform thermal averaging on the right hand side of Eq. (19), we follow the general approach described in Ref. [16]. First of all, in the spirit of the effective field theory, multispin correlation functions are approximated by products of single spin averages. We then take advantage of the integral representation of the Dirac's delta distribution, in order to write Eq. (19) in the following form
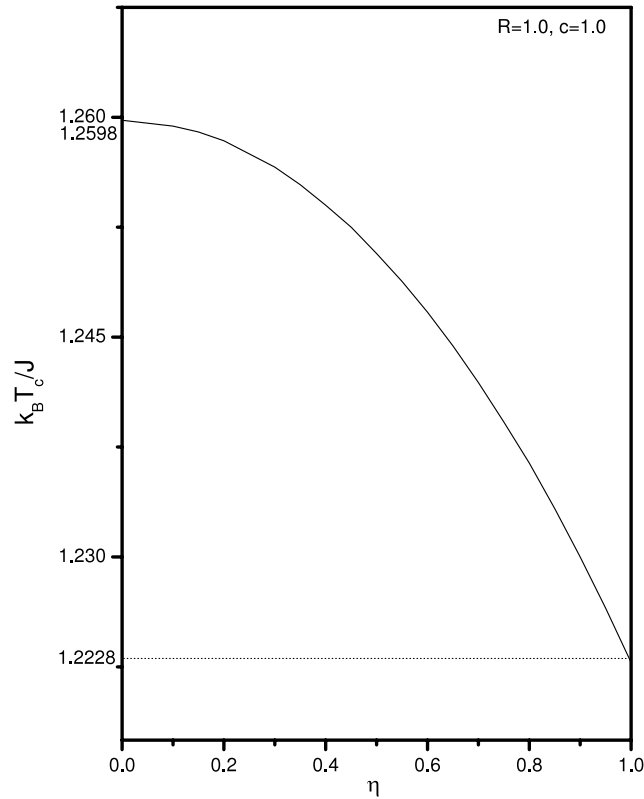
Fig. 3. Dependence of the Curie temperature on the reduced exchange anisotropic parameter η for $c = 1.0$ and $R = 1.0$.

$$m_{nz} = \int d\omega f_z(\omega) \frac{1}{2\pi} \int \left[dt \exp(i\omega t) \prod_j \langle \exp(it J_{ij}\sigma_{jz}) \rangle \right].$$ (20)

Now, we introduce the probability distribution of the spin variables (for details see Ref. [16])

$$P(S_{iz}, c) = \frac{1}{2}(1-c)\delta(c_n) \left[\delta\left(S_{nz} + \frac{1}{2}\right) + \delta\left(S_{nz} - \frac{1}{2}\right) \right]$$

$$+ \frac{1}{2}\delta(c_n - 1) \left[(c - 2m_{nz})\delta\left(S_{nz} + \frac{1}{2}\right) + (c + 2m_{nz})\delta\left(S_{nz} - \frac{1}{2}\right) \right].$$ (21)

Using the four previous equations, we get the following equations for the layer magnetization

$$m_z = c2^{2-2N} \sum_{\mu=0}^{N-1} \sum_{\mu_1=0}^{N-1-\mu} \sum_{\nu=0}^{N-1} \sum_{\nu_1=0}^{N-1-\nu} \left\{ C_\mu^{N-1} C_{\mu_1}^{N-1-\mu} C_\nu^{N-1} C_{\nu_1}^{N-1-\nu} (1-c)^{\nu+\mu} 2^{(-\mu-\nu)} \right.$$

$$\left. \times (c - 2m_z)^{\mu_1+\nu_1} (c + 2m_z)^{2(N-1)-(\mu_1+\nu_1+\nu+\mu)} \right\} f_z\left(\beta\frac{J}{2}(N-1-\mu-2\mu_1), \beta\frac{J}{2}(N-1-\nu-2\nu_1) \right).$$ (22)

In these equations, the case of a simple cubic lattice which is considered ($N = 6$) and C_k^l are the binomial coefficients, $C_k^l = \frac{k!}{l!(k-l)!}$.

We have thus obtained the self-consistent equation (22) for the magnetization m_z, that can be solved directly by numerical iteration. No further algebraic manipulation is necessary. This is the advantage of introducing the probability distribution technique.

3. Results and discussion

Let us begin with the evaluation of the critical temperature $k_B T_c/J$ versus the $(1-c)$ Al concentration. The Curie temperature $k_B T_c/J$ is determined as the lowest temperature at which Eq. (22) has a nontrivial solution $m_z \neq 0$. In other
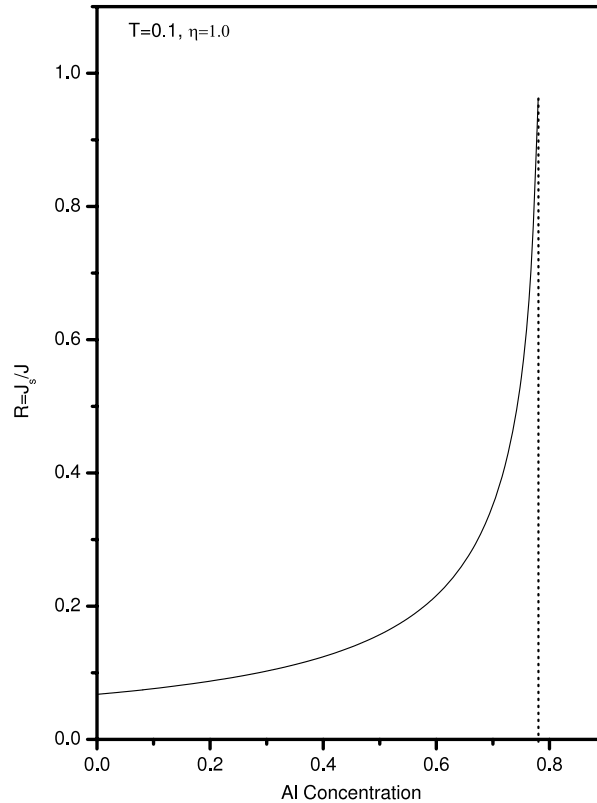
Fig. 4. The interaction parameter R dependence of the $(1 - c)$ Al concentration. The parameters adopted here are $T = 0.1$ and $\eta = 1.0$.

words, when Eq. (22) is expanded into power series of m_z, the coefficient of the linear term of m_z on the right-hand side is equal to unity at T_c. Thus the equation for T_c becomes

$$a = 1 \tag{23}$$

where

$$
\begin{aligned}
a = 2^{-2N+2} \sum_{\mu=0}^{N-1} \sum_{\mu_1=0}^{N-1-\mu} \sum_{\nu=0}^{N-1} \sum_{\nu_1=0}^{N-1-\nu} \sum_{i_1=0}^{\mu_1+\nu_1} \sum_{i_2=0}^{2N-2-(\mu+\nu+\mu_1+\nu_1)} C_\mu^{N-1} C_{\mu_1}^{N-1-\mu} C_\nu^{N-1} C_{\nu_1}^{N-1-\nu} \\
\times C_{i_1}^{\mu_1+\nu_1} C_{i_2}^{2N-2-(\mu+\nu+\mu_1+\nu_1)} (1-c)^{\nu+\mu} 2^{\mu+\nu+i_1+i_2} c^{2N-(\mu+\nu+i_1+i_2+1)} (-1)^{i_1} \\
\times \delta_{i_1+i_2,1} f_z \left(\beta \frac{J}{2}(N-1-\mu-2\mu_1), \beta \frac{J}{2}(N-1-\nu-2\nu_1) \right).
\end{aligned} \tag{24}
$$

The dependence of the critical temperature on the $(1 - c)$ Al concentration is shown in Fig. 1. The curves correspond to the Heisenberg model ($\eta = 1$), and for different values of the parameter $R = J_s/J$. We see that for this model, with the increasing of the value of concentration $(1 - c)$ of magnetic atom of Al, the phase diagram in which the ferromagnetic ordering is realizable gradually becomes small and goes to a low value at the critical concentration, and near of this value the critical temperature is independent of the parameter R.

The dependence of the critical temperature on the reduced exchange anisotropic parameter η is shown in Fig. 2 for different values of concentration c. As expected for different values of concentration c, with the increasing the value of the anisotropic parameter η, the critical temperature $k_B T_c/J$ decreases and its start from different values of $k_B T_c/J$ depending on the value of Al concentration.

In Fig. 3, and in particular for the pure case we have plotted the dependence of the critical temperature on the reduced exchange anisotropic parameter. The critical temperature T_c decreases from its Ising value $k_B T_c/J = 1.2598$ ($\eta = 0$) with the increase of η to reach its lowest value which is the Heisenberg value at $k_B T_c/J = 1.2228$ ($\eta = 1$). Our results are in agreement with those of Idogaki et al. [19] and Wu et al. [20]. (Because $\overrightarrow{S}^2 = \frac{1}{4}$, our numerical values are $\frac{1}{4}$ their values).
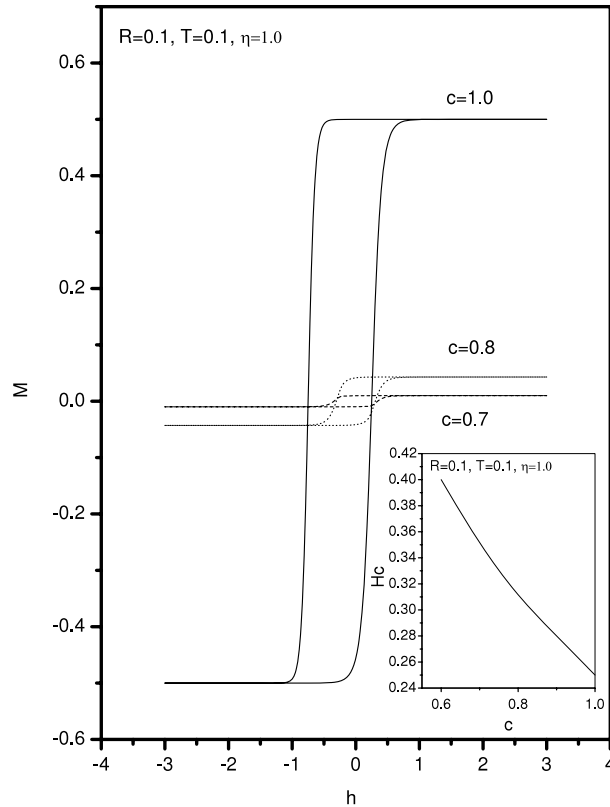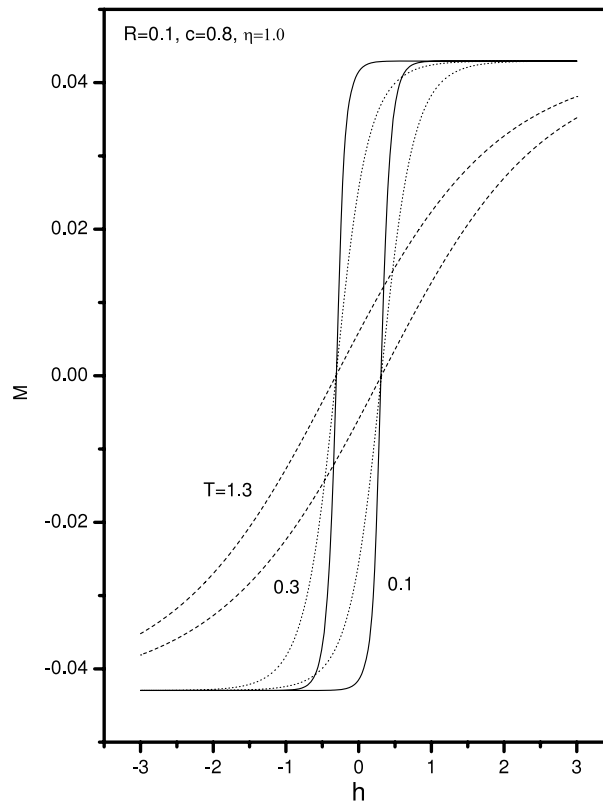
Fig. 5. The longitudinal magnetic field dependence of the spontaneous magnetization for different value of concentration c. Solid, dotted and dashed lines correspond to the value of concentration $c = 1.0$, 0.8 and 0.7 respectively. The parameters adopted here are $R = 0.1$, $\eta = 1.0$ and $T = 0.1$.

Fig. 4 shows the calculated $R = J_s/J$ as a function of the Al concentration. It can be noted that the parameter R increases slowly from a value near one for low concentration $(1 - c)$ and then increases rapidly near the critical concentration $(1 - c) \simeq 0.78$.

Fig. 5 shows the hysteresis loops evaluated at $T = 0.1$ and $R = 0.1$ for these disordered alloys. From these, one can see that this is a soft magnetic material. The $(M-h)$ ferromagnetic hysteresis loops are obtained by changing cyclically the value of the magnetic field for different values of the concentration c of Fe atoms. The hysteresis loops obtained indicate, the transition from the paramagnetic to ferromagnetic state. We can see in Fig. 5 that the magnetization curves are symmetric for both positive and negative longitudinal fields and the hysteresis loops are more influenced by the value of the concentration, in particular for the low values of longitudinal field from the pure to the diluted case respectively and also with increasing the value of concentration c, the saturation increases, which also suggests that a ferromagnetic coupling indeed should be expected between the Fe and Al atoms. Inset of Fig. 5, we have plotted the dependence of the coercive field on the value of concentration c, we can see that by increasing the value of concentration c, the coercive field H_c decreases. This reduction on the coercive field due to the collective response of the magnetic moments that lead to a reduction of the energy barrier for magnetization reversal. In Fig. 6, we plot the magnetization dependence of the longitudinal magnetic field, by changing the value of the temperature T. For these curves, the hysteresis loops are regular and symmetrical, whereas at low temperature and magnetic field h the curves tend to the same value of saturation.

4. Conclusion

In conclusion, we have studied the phase diagrams and some magnetic properties of the ferromagnetic site-diluted quantum Heisenberg model applied to the disordered Al–Fe alloys, using the effective field theory based on the probability distribution technique. From this study, we have investigated the influence of the reduced exchange anisotropic parameter η and $(1 - c)$ Al concentration on the critical temperature and magnetization profiles. We can see that the present model, although simple, can give a satisfactory description of Al–Fe alloys in the disordered phase. Moreover, from this theoretical point of view, just for the parameters R and η, the present model can account for the main magnetic properties of these disordered alloys such as the hysteresis loops and the coercive field found for some typical values of concentration c, R and the anisotropic parameter η.

Fig. 6. The longitudinal field dependence of the spontaneous magnetization for different values of temperatures T. Solid, dotted and dashed lines correspond to the value of temperature $T = 1.3$, 0.3 and 0.1 respectively. The parameters adopted here are $R = 0.1$, $\eta = 1.0$ and $c = 0.8$.

Acknowledgements

References

[1] M.N. Baibich, J.M. Broto, A. Fert, F. Nguyen Van Dau, F. Petroff, P. Eitenne, G. Creuzet, A. Friedrich, J. Chazelas, Phys. Rev. Lett. 61 (1988) 2472.
[2] G. Binash, P. Grünbeg, F. Saurenbach, W. Zinn, Phys. Rev. B 39 (1988) 4828.
[3] R. Stinchcombe, in: C. Domb, M.S. Green (Eds.), Phase Transitions and Critical Phenomena, Academic, London, 1982.
[4] J. Restrepo, G.A. Pérez Alcázar, J.M. Gonzalez, J. Appl. Phys. 83 (1998) 7249.
[5] G.A. Pérez Alcázar, J.A. Plascak, E. Galvão da Silva, Phys. Rev. B 34 (1986) 1940.
[6] M. Salazar, Ligia E. Zamora, G.A. Pérez Alcázar, J.A. Plascak, W.R. Aguirre, Physica B 320 (2002) 236.
[7] J.A. Plascak, W. Figueiredo, B.C.S. Grande, Braz. J. Phys. 29 (1999) 579.
[8] L.G. Ferreira, S.R. Salinas, M.J. Oliveira, Phys. Status Solidi B 83 (1979) 229.
[9] H. Sato, A. Arrot, Phys. Rev. 114 (1959) 1427.
[10] J. Pickart, R. Nathans, Phys. Rev. 123 (1961) 1163.
[11] P. Shukla, M. Wortis, Phys. Rev. B 21 (1980) 159.
[12] G.S. Grest, Phys. Rev. B 21 (1980) 165.
[13] G.A. Perez, E. Galvao da Silva, J. Phys. F: Met.Phys. 17 (1987) 2323.
[14] N. Moreno, F.C. Montenegro, Phys. Rev. B 56 (1997) 14567.
[15] M. Salazar, Ligia E. Zamora, G.A. Pérez Alcazar, J.A. Plascak, W.R. Aguirre, Physica B 320 (2002) 236.
[16] M. Saber, Chin. J. Phys. 35 (1997) 577.
[17] A. Bobak, M. Jascur, Phys. Stat. Solidi (b) 135 (1986) k9.
[18] J. Mielnicki, G. Wiatrowski, T. Balcerzak, J. Magn. Magn. Mater. 71 (1988) 186.
[19] T. Idogaki, Y. Miyoshi, J.W. Tucker, J. Magn. Magn. Mater. 154 (1996) 221.
[20] Y.Z. Wu, Z.Y. Li, Solid State Commun. 106 (1998) 789.